Energy Conversion and Management 98 (2015) 533–543

Contents lists available at ScienceDirect

Energy Conversion and Management

journal homepage: www.elsevier.com/locate/enconman

Hierarchical energy and frequency security pricing in a smart microgrid: An equilibrium-inspired epsilon constraint based multi-objective decision making approach

Navid Rezaei, Mohsen Kalantar *

Center of excellence for Power Systems Automation and Operation, Electrical Engineering Department, Iran University of Science and Technology (IUST), Tehran, Narmak 16846 13114, Iran

ARTICLE INFO

Article history:
Received 10 February 2015
Accepted 2 April 2015

Keywords:
Smart microgrid
Hierarchical reserve management
Security pricing
Multi-objective optimization
Nash equilibrium point

ABSTRACT

The present paper formulates a frequency security constrained energy management system for an islanded microgrid. Static and dynamic securities of the microgrids have been modeled in depth based on droop control paradigm. The derived frequency dependent modeling is incorporated into a multi-objective energy management system. Microgrid central controller is in charge to determine optimal prices of energy and frequency security such that technical, economic and environmental targets are satisfied simultaneously. The associated prices are extracted based on calculating related Lagrange multipliers corresponding to providing the microgrid hourly energy and reserve requirements. Besides, to generate optimal Pareto solutions of the proposed multi-objective framework augmented epsilon constraint method is applied. Moreover, a novel methodology on the basis of Nash equilibrium strategy is devised and employed to select the best compromise solution from the generated Pareto front. Comprehensive analysis tool is implemented in a typical test microgrid and executed over a 24 h scheduling time horizon. The energy, primary and secondary frequency control reserves have been scheduled appropriately in three different case-studies which are defined based on the microgrid various operational policies. The optimization results verify that the operational policies adopted by means of the microgrid central controller have direct impacts on determined energy and security prices. The illustrative implementations can give the microgrid central controller an insight view to provide an appropriate trade-off between the microgrid security requirements and economic-environmental objectives.

1. Introduction

1.1. Motivations

By ever-increasing integration of intermittent Renewable Energy Sources (RESs) and inertia less Voltage Source Inverter (VSI) based Distributed Generations (DGs), maintaining the real-time power balance between load and generation is an important control task which must be effectively fulfilled by means of the power system operators [1]. The disturbances in the power balance lead the system frequency to be deviated from its nominal set-point [2]. Owing to lesser inertia and limited pool of available ancillary service resources, the frequency security of islanded renewable based inverter interfaced microgrids is subjected to higher risks which require adequately provision of frequency control reserves. Hence, the associated costs of the frequency regulation services are predicted to rise significantly. Thus, Microgrid Central Controller (MGCC) should manage the frequency security with reasonable operating cost and also owing to environmental policies [3].

The VSI-based DGs can mimic the load-frequency control functions of the synchronous generators based on the droop controllers. The frequency control functions of a microgrid can be achieved through a hierarchical control structure. This brings into sharp focus the need to an in-depth modeling of the corresponding frequency control functions of the VSI-based DGs and also efficient incorporation of the associated mathematical formulations into microgrid energy management system [4]. Therefore, it seems to be necessary that the MGCC as the highest control level in the islanded microgrids, takes an effective methodology to optimistically determine the associated prices of the energy and security. Motivated by this need, this paper aims in the light of comprehensive modeling of the static and dynamic frequency control functions of the droop controlled VSI-based microgrids, to bring

* Corresponding author. Tel.: +98 2173225662; fax: +98 2173225662.
E-mail addresses: nrezaei@iust.ac.ir (N. Rezaei), kalantar@iust.ac.ir (M. Kalantar).

http://dx.doi.org/10.1016/j.enconman.2015.04.004
0196-8904/

Nomenclature

Indices

i	index of VSI based DG from 1 to *Ng*
w	index of wind turbines from 1 to *Nw*
v	index of photovoltaic panels from 1 to *Nv*
d	index of demand response providers from 1 to *Nd*
s	index of random scenarios from 1 to *Ns*
h	index of hours from 1 to *Nh*
l	index of frequency control level could be *pri* (primary) and *sec* (secondary)
ud	index of scheduled reserves could be *up* or *down*

Acronyms

DER	Distributed Energy Resource
DG	Distributed Generation
DR	Demand Response
DRP	Demand Response Provider
ELNS	Expected Load Not Supplied
MCS	Monte Carlo Simulation
MGCC	Micro Grid Central Controller
MILP	Mixed-Integer Linear Programming
PV	Photovoltaic
RES	Renewable Energy Source
RWM	Roulette Wheel Mechanism
VSI	Voltage Source Inverter
WT	Wind Turbine

forward an appropriate methodology to specify the hourly prices of the energy and security provision of the islanded microgrids. An appropriate pricing mechanism can give the MGCC an insight view to promote the microgrid optimal energy and security management.

1.2. Literature review and approach

In the literature, the concept of the microgrid energy management has been explored from the technical, economic and environmental friendly viewpoints using either single or multi-objective optimization frameworks. Chen et al. [5] presented a smart energy management system to investigate cost optimization problem of a microgrid under different operational policies in either grid connected or islanded modes. Mohammad et al. [6] applied a heuristic based algorithm to a non-linear economic dispatch problem of a microgrid. The optimal power flow problem of an islanded microgrid has been solved effectively in [7] subject to the loadability and associated droop control constraints. However, the frequency dependent control functions of the droop controlled DGs and their direct impacts on the microgrid energy and reserve scheduling have not been explored. Authors in [8], proposed a hierarchical microgrid energy management system by appropriate modeling the primary and secondary control functions of the local controllers and also the MGCC. However, the potential of the Demand Response Providers (DRP) as one of main components of the smart microgrids was not modeled in the proposed frequency control approach. Besides, no attention was paid to the uncertainty effects associated to the RESs and/or load fluctuations. Ref. [9], proposed a two-stage scenario-based stochastic programming to efficiently manage the operational planning of a fuel cell based microgrid. The heuristic based cuckoo optimization algorithm was employed in the optimization module. Authors in [10], have adopted non dominated sorting genetic algorithm to solve a multi-objective economic-environmental energy dispatch in a stand-alone microgrid. The chance-constraint methodology was used to describe the system uncertainties. Despite that methodologies may be effective their solutions may be affected by the drawback of the meta-heuristic algorithms in handling with high constrained problems. In [11] energy management problem of an islanded microgrid has been carried out using mixed integer non-linear programming approach to optimize the utilization of Distributed Energy Resources (DERs) with a cheap day-ahead operational cost. Mazidi et al. [12] explored a coordinated approach of DRPs and DGs to manage the microgrid uncertainties while the operational costs have been minimized. As well in [13], using some DRPs, the end-user consumers have been participated into the microgrid energy and reserve scheduling. Indeed, if the DRPs' bids have been accepted, they were called to participate into operational planning by adjusting their power consumption. Despite the efficiency of the proposed approaches none of the above mentioned papers were taken into account the frequency dependent model of the droop controlled DGs. They only focus on the secondary control functions of the MGCC and the great impacts of the primary control reserves in operational planning of the microgrids were disregarded. Recently, in [14] a novel cost-effective frequency aware energy management system has been proposed. Under a single objective portfolio, the day-ahead primary and secondary control reserves have been managed properly such that the microgrid static frequency security was managed owing to the MGCC economic and environmental constraints. In [14], the authors concentrated on only the static performance of the VSI-based DGs and no solution was proposed to cope with the low inertia stack of the islanded microgrids. Noteworthy, the low inertia of the VSI-based DGs can have deteriorative impacts on the islanded microgrid dynamic security which should be considered by means of the hierarchical frequency control structure. Motivated by this need, in [15] in order to manage the dynamic security of the microgrids, Rate Of Change Of Frequency (ROCOF) function of the droop controlled DGs has been formulated in-detail based on the proposed virtual inertia concept. The derived formulations were conducted by means of the MGCC who executing a security constrained unit commitment problem to schedule the day-ahead energy and hierarchical reserve resources. In [14,15] the hourly prices of energy and frequency security have not been extracted.

By reviewing the literature, the lacuna of a comprehensive energy management system which optimizes the operational planning subject to technical, economic and environmental objectives and determines the associated prices of energy and security is still evident. Therefore, contributing to references [14,15], the present paper proposes a hierarchical energy management system which precisely considers the static and dynamic frequency control functions of the microgrids and aims to determine associated optimal prices of the energy and security. The MGCC continuously monitors the static and dynamic frequency profiles of the islanded microgrid and optimizes the microgrid operational planning by properly adjusting the reference power settings of the droop controlled DGs. Owing to operational policies the MGCC can restore the microgrid frequency either at exactly rated value or allows the frequency to be deviated in secure ranges.

Within the above context, the main contributions of this paper can be presented as the following:

- A comprehensive frequency dependent multi-objective energy management system is presented. It is aimed to solve the energy and hierarchical reserve management problem of a droop controlled islanded microgrid such that the technical, economic and environmental targets are optimized simultaneously. To generate the optimal Pareto solutions of the proposed multi-objective framework the well known efficient epsilon constraint method is applied. Moreover, a novel methodology on the basis of the Nash equilibrium strategy is devised and employed to select the best compromise solution from the generated Pareto front.
- The hourly prices of the energy and security of an islanded microgrid are derived using an efficient methodology. The associated prices of security are derived under different operational policies during which the impacts of participating the demand response programs can be investigated thoroughly. Moreover, the effects of managing the frequency at a wider security range can be reflected in the specified prices of the microgrid security. Furthermore, day-ahead energy and reserve resources are scheduled appropriately. Besides, under a coordinated approach, the DRP are actively participated in providing secondary control reserves.

The remainder of the paper is divided into the following sections: Section 2, formulates an efficient mixed integer linear programming (MILP)-based modeling of the proposed hierarchical frequency control structure. In Section 3, the proposed modeling is simulated in an islanded microgrid and illustrative implementations are analyzed in-detail. Lastly, Section 4 concludes the paper.

2. Formulations

In this section, mathematical modeling of the proposed hierarchical energy management system is formulated comprehensively. The proposed hierarchical frequency control structure in an islanded microgrid is illustrated in Fig. 1.

Observably, the MGCC optimizes the operational planning of the microgrid by appropriately managing the power set-points of the dispatchable VSI-based DGs. Indeed, the MGCC assures the microgrid frequency security in front of Wind Turbines (WTs), Photovoltaic (PV), load fluctuations and DG possible outages. Furthermore, the droop controlled DGs are in charge to manage the microgrid primary frequency excursions in the line of the MGCC control commands and in proportion to the droop characteristics. Worth mentioning that the RES units, i.e. WTs and PVs are not participated into the frequency control structure, however the MGCC should appropriately takes into account the associated intermittencies. It is also assumed that the end user consumers can actively participate into the secondary frequency control of the microgrid in the light of the demand response programs.

2.1. Droop controlled VSI-based DGs

2.1.1. Primary control level

The primary frequency control functions are performed using the VSI based droop controlled DGs in a distributed and automatic manner [16]. The DGs release their scheduled primary control reserves in proportion to their droop characteristics and in accordance to the microgrid primary frequency excursions. Notably, the direct coupling between the microgrid frequency and scheduling the primary control reserves highlights the necessity of the modeling the frequency dependent behavior of the microgrids [17,18]. With respect to the secondary control reserves which are mainly scheduled based on the power capacity and ramp-rates of the DGs, scheduling of the primary control reserves should executed owing to the steady-state frequency profile of the microgrids [19]. In the following the detailed block-diagram of a VSI-based droop controlled VSI-based DG in the steady-state is presented by Fig. 2.

The control functions corresponding to the internal voltage and current controllers have been neglected in the steady-state. It is also assumed that all the formulations are constructed based on the steady-state modeling. As mentioned, in an islanded microgrid, the frequency excursions can easily be occurred due to unpredictable behaviors of the WTs and PVs as well as the random load demand fluctuations. Besides, the possible contingencies stem from the DG unit outages can also lead the microgrid frequency

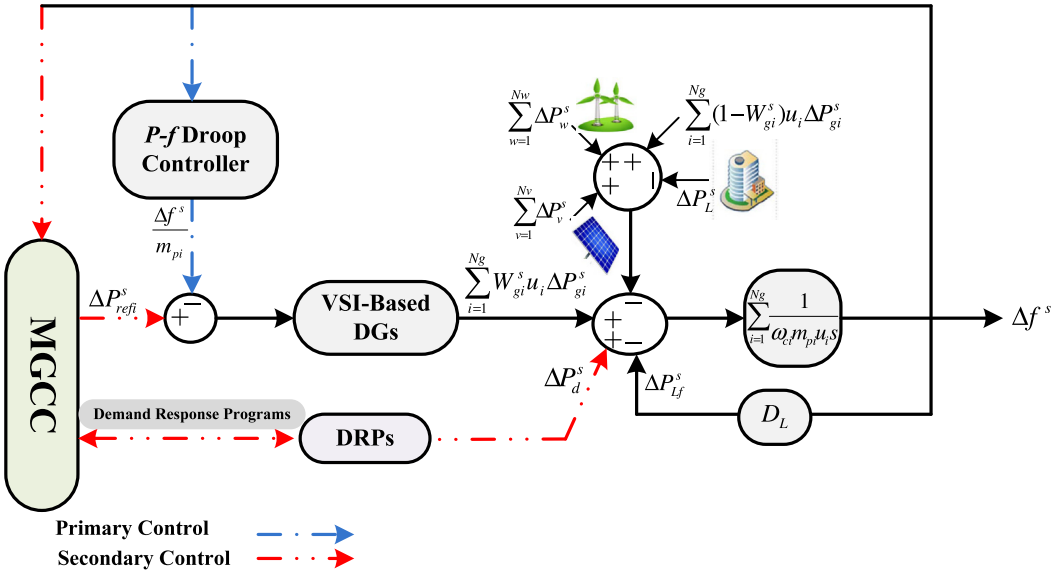

Fig. 1. Diagram of microgrid hierarchical control structure.

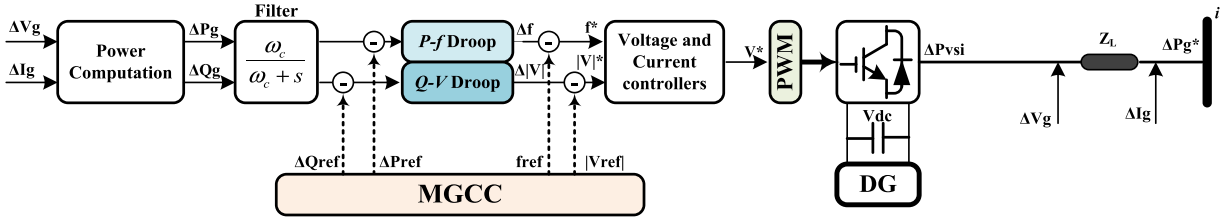

Fig. 2. The detailed block-diagram of a droop controlled VSI-based DG.

to be deviated from its nominal value. Thus, the droop controlled DGs must change their active power outputs to control the frequency excursions. Therefore, owing to Figs. 1 and 2, the performances of the available droop controlled DGs can be formulated as follows in Eq. (1):

$$\sum_{i=1}^{Ng} W^s_{i,h}\cdot\Delta P^s_{i,l,h} = \Delta P^s_{L,l,h} - \sum_{w=1}^{Nw}\Delta P^s_{w,l,h} - \sum_{v=1}^{Nv}\Delta P^s_{v,l,h} - \sum_{i=1}^{Ng}(1-W^s_{i,h})\cdot\Delta P^s_{i,l,h} - \sum_{d=1}^{Nd}\Delta P^s_{d,l,h} + D^s_{L,l,h}\cdot\Delta f^s_{l,h} - LSH^s_{l,h} \quad (1)$$

where $\Delta P^s_{i,l,h}, \Delta P^s_{w,l,h}, \Delta P^s_{v,l,h}, \Delta P^s_{d,l,h}, \Delta P^s_{L,l,h}$ are indicating active power deviation of ith VSI based DG, active power deviation of wind turbine w, active power deviation of photovoltaic panel v, offered load reduction variation corresponding to dth DRP and microgrid load consumption deviation in scenario s, control level l and hour h, respectively. $\Delta f^s_{l,h}$ and $LSH^s_{l,h}$ represent microgrid frequency excursion and load to be shed unwillingly in scenario s, control level l at hour h, respectively. $D^s_{L,l,h}$ indicates frequency elasticity of microgrid total loads in scenario s, control level l and hour h. $W^s_{i,h}$ is a binary variable indicating availability status of ith DG at hour h in scenario s. The value 0 corresponds to the condition in which the DG is out of service.

According to Fig. 2, the precise static control function of the droop controlled VSI can be formulated as follows in Eq. (2):

$$W^s_{i,h}\cdot m_{p,i}\cdot\left(\Delta P^s_{i,l,h} - \Delta P^s_{ref,i,l,h}\right) = W^s_{i,h}\cdot u^l_{i,h}\cdot\left(\Delta f^s_{ref,l,h} - \Delta f^s_{l,h}\right) \quad (2)$$

where $\Delta P^s_{ref,i,l,h}$ and $\Delta f^s_{ref,l,h}$ show reference power deviation of ith VSI based DG and microgrid reference frequency in scenario s, control level l and hour h, respectively. $u^l_{i,h}$ stands for binary variable indicating commitment state of ith VSI based DG at hour h and control level l. $m_{p,i}$ represents frequency droop control gain parameter of ith VSI-based DG. Worth mentioning that the reference values of the active power set-points and also the frequency reference value are adjusted by means of the MGCC. Therefore, due to time limitation during the primary control level in which the primary frequency control functions are performed within a few seconds, the MGCC has not adequate time to make decision on adjusting the microgrid reference values. Likewise, the commitment states of the DGs are remained unchanged during the primary control level. Eqs. (3)–(5) characterizing that during the primary control level, the reference values and the commitment states of the DGs are as the same as their scheduled values.

$$W^s_{i,h}\cdot P^s_{ref,i,l,h}\Big|_{l=pri} = W^s_{i,h}.P_{i,h}\cdot u_{i,h} \quad (3)$$

$$f^s_{ref,l,h}\Big|_{l=pri} = f_{ref,h} = f_{ref} \quad (4)$$

$$W^s_{i,h}\cdot u^l_{i,h}\Big|_{l=pri} = W^s_{i,h}\cdot u_{i,h} \quad (5)$$

where $P^s_{ref,i,l,h}$ represents reference power set-point of ith VSI based DG in scenario s, control level l and hour h. $P_{i,h}$ and $u_{i,h}$ denote active power output and commitment state of ith VSI based DG at hour h. Therefore, the detailed time domain frequency control function of the proposed droop controlled VSI-based DG during the primary control level can be presented by Eq. (6):

$$W^s_{i,h}\cdot m_{p,i}\cdot\Delta P^s_{i,l,h} = -W^s_{i,h}\cdot u^l_{i,h}\cdot\left\{\frac{1}{\omega_{c,i}}\frac{d(\Delta f^s_{l,h})}{dt} - \Delta f^s_{l,h}\right\},\ l = pri \quad (6)$$

where $\omega_{c,i}$ shows low-pass filter cut-off frequency parameter of ith VSI based DG. Apart from the first few seconds of the primary control level, it can be assumed that the transients and the oscillating modes are negligible, i.e. according to Eq. (7), the dynamic control function can be neglected.

$$\frac{d\Delta f^s_{l,h}}{dt}\approx 0,\ l = pri \quad (7)$$

Therefore, owing to Eq. (7), Eq. (8) can be simply concluded from Eq. (6):

$$W^s_{i,h}\cdot m_{p,i}\cdot\Delta P^s_{i,l,h} = -W^s_{i,h}\cdot u^l_{i,h}\cdot\Delta f^s_{l,h},\ l = pri \quad (8)$$

The static frequency control function of the droop controlled VSI-based DG can be expressed according to Eq. (8). To describe the dynamic frequency control function of the droop controlled VSI-based DG during the first few seconds, the control function corresponding to the static modeling can be disregarded, therefore Eq. (6) can be approximately simplified as follows in Eq. (9):

$$W^s_{i,h}\cdot m_{p,i}\cdot\Delta P^s_{i,l,h}\approx -W^s_{i,h}\cdot u^l_{i,h}\cdot\left\{\frac{1}{\omega_{c,i}}\frac{d(\Delta f^s_{l,h})}{dt}\right\},\ l = pri \quad (9)$$

Since the microgrid reference frequency equals to the scheduled value during the primary control level, Eq. (10) can be concluded:

$$\frac{d(\Delta f^s_{l,h})}{dt} = \frac{d(f^s_{l,h} - f^s_{ref,l,h})}{dt} = \frac{df^s_{l,h}}{dt},\ l = pri \quad (10)$$

According to Eqs. (9) and (10), (11) clearly represents the dynamic frequency control function of the droop controlled VSI-based DG.

$$W^s_{i,h}\cdot u^l_{i,h}\cdot\left\{\frac{1}{\omega_{c,i}m_{p,i}}\frac{df^s_{l,h}}{dt}\right\}\approx -W^s_{i,h}\cdot\Delta P^s_{i,l,h},\ l = pri \quad (11)$$

As a result, Rate of Change of Frequency (ROCOF) of the ith VSI-based DG with the rated power P_{rated} can be approximately calculated using Eq. (12):

$$W^s_{i,h}\cdot u^l_{i,h}\cdot ROCOF^s_{i,h}\approx W^s_{i,h}.u^l_{i,h}.\frac{df^s_{l,h}}{dt} = -\frac{f_{ref}\cdot W^s_{i,h}\cdot\omega_{c,i}\cdot m_{p,i}\cdot\Delta P^s_{i,l,h}}{P_{rated,i}},\ l = pri \quad (12)$$

where $ROCOF^s_{i,h}$ explains rate of change of frequency of ith VSI-based DG in scenario s at hour h. Eq. (12) can also be calculated for the whole microgrid as follows in Eq. (13):

$$ROCOF^{s}_{MG,h} \approx -\left(\frac{f_{ref}\sum_{i=1}^{Ng} W^{s}_{i,h}\cdot \Delta P^{s}_{i,l,h}}{\sum_{i=1}^{Ng} W^{s}_{i,h}\cdot \frac{1}{\omega_{c,i}\cdot m_{p,i}}\cdot P_{rated,i}\cdot u^{l}_{i,h}}\right),\ l = pri \tag{13}$$

where $ROCOF^{s}_{MG,h}$ approximately explains rate of change of frequency of the whole microgrid in scenario s at hour h.

2.1.2. Secondary control level

The MGCC should provide the reliable operation of the microgrid by ensuring the static and dynamic frequency security indices lies into the safe ranges. The MGCC can readjust the active power set-points of the VSI-based DGs such that the microgrid secondary frequency is either managed at exactly the nominal value or controlled at a more secure range. Noticeably, the frequency restoration function of the MGCC should be carried out subject to the microgrid economic and environmental targets. According to Fig. 2, the MGCC frequency control function during the secondary level can be formulated by Eq. (14):

$$P^{s}_{i,l,h} = W^{s}_{i,h}\cdot u^{l}_{i,h}\cdot\left\{P^{s}_{ref,i,l,h} - \frac{1}{m_{p,i}}\left(f^{s}_{l,h} - f_{ref}\right)\right\},\ l = \sec \tag{14}$$

From Eqs. (1), (8) and (14) the microgrid primary and secondary frequency excursions can take the form of Eqs. (15) and (16):

$$\Delta f^{s}_{l,h}\Big|_{l=pri} = -\frac{\Delta P^{s}_{L,l,h} - \sum_{w=1}^{Nw}\Delta P^{s}_{w,l,h} - \sum_{v=1}^{Nv}\Delta P^{s}_{v,l,h} - \sum_{i=1}^{Ng}(1-W^{s}_{i,h})\cdot\Delta P^{s}_{i,l,h} - \sum_{d=1}^{Nd}\Delta P^{s}_{d,l,h} - LSH^{s}_{l,h}(l,h)}{D^{s}_{L,l,h} + \sum_{i=1}^{Ng}\frac{1}{m_{p,i}}\cdot W^{s}_{i,h}\cdot u^{l}_{i,h}} \tag{15}$$

$$\Delta f^{s}_{l,h}\Big|_{l=\sec} = \frac{\sum_{i=1}^{Ng} W^{s}_{i,h}\cdot\left[P^{s}_{ref,i,l,h} - P^{s}_{i,l,h}\right]}{D^{s}_{L,l,h} + \sum_{i=1}^{Ng}\frac{1}{m_{p,i}}\cdot W^{s}_{i,h}\cdot u^{l}_{i,h}},\ l = \sec \tag{16}$$

2.2. Demand response resources

One of the main microgrid contributors are DRPs. DRPs can represent commodious and efficient energy services through alerting in end-user consumption patterns [20]. Therefore, the MGCC can provide a coordinated control together with the DGs to promote the microgrid reliability and security with consideration to the economic and environmental targets. Based on the more dispatchable capability of the demand bidding and ancillary service programs, the present paper aims to apply them into the microgrid energy management system [21]. For this purpose, DRPs are employed to submit demand reduction offers to the MGCC. The accepted offers are called to reduce the suggested demand. Obviously, the proposed DR programs are incorporated into the secondary control level and can be utilized for both energy and reserve provision. Indeed, in the primary control level, due to the time limitation, it seems that without any advanced metering infrastructure or smart frequency aware controller it may not possible to schedule the microgrid loads for participating into the primary frequency control [22]. In this paper, the proposed secondary DR programs are modeled using a step-wise price-demand curve as presented in by Fig. 3 [15]. C1, C2, C3 and C4 are associated offered prices corresponding to P1, P2, P3 and P4 load reduction offers, respectively.

2.3. Scenario generation and reduction

To manage uncertainty resources of the microgrid a two-stage scenario based stochastic programming is implemented. To generate associated scenarios the well-known Monte-Carlo Simulation (MCS) and Roulette Wheel Mechanism (RWM) strategies are applied to corresponding Probability Density Functions (PDFs) of the WT/PV and load demands [23]. Depending on desired accuracy, corresponding PDFs are divided to a number of discrete intervals

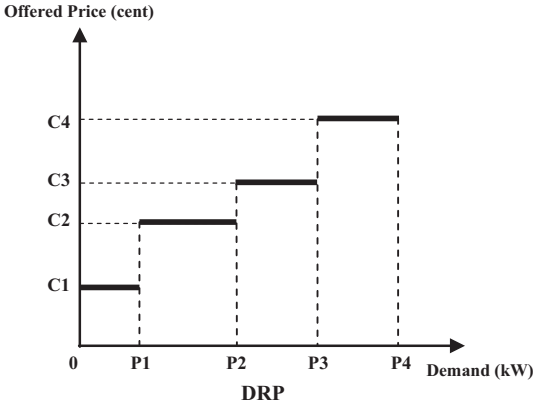

Fig. 3. Demand-price offer package.

with different probability levels [24]. Each discretized interval corresponds to a specified error value with respect to the forecasted power generation and load consumption. The RWM strategy models the stochastic level of each interval. Each interval throughout the roulette wheel indicates a specific forecasting error. The probabilities of the intervals on the roulette wheel are normalized such that their summation equals to unity. Finally, a scenario is generated by comparing a random number produced using the MCS, between 0 and 1, to the normalized intervals on the RWM path. Each interval on the roulette wheel in which the generated random number falls is corresponding to a scenario. An analogous approach based on the MCS and RWM is also performed to generate the random scenarios associated to DG possible outages. The MCS produced random number between 0 and 1 is compared to Forced Outage Rate (FOR) of each DG. If the generated random number is smaller than the associated FOR, the DG is in service. After that the required numbers of the scenarios have been generated, a proper scenario reduction algorithm is applied to attain a trade-off between the computational efficiency and the solution accuracy based on removing the low probable and similar scenarios [25]. Each of remained scenarios should be solved deterministically owing to its probability. Finally, to find out the expected result of the problem and simplification of the solution interpretation, obtained solutions from the reduced scenarios are aggregated according to their normalized probability. Further description can be found in [14,19].

2.4. Multi-objective hierarchical frequency management system

2.4.1. Objective functions

In the proposed multi-objective frequency management problem, four objective functions are considered including total cost (F_1), total emission (F_2), expected value of total frequency excursions (F_3) and expected value of rate of change of frequency (F_4) of the microgrid day-ahead operational planning. Eq. (17) explains the microgrid total operational cost corresponding to the energy and reserve management.

$$\begin{aligned} F_1 = \sum_{h=1}^{Nh}\Bigg(&\sum_{i=1}^{Ng}\left[a_i\cdot u_{i,h} + b_i\cdot P_{i,h}\right] + \rho_w\cdot\sum_{w=1}^{Nw}P_{w,h} + \rho_v\cdot\sum_{v=1}^{Nv}P_{v,h} \\ &+ \sum_{d=1}^{Nd}\rho^{E}_{d}\cdot P_{d,h} + \sum_{i=1}^{Ng}\sum_{l}\sum_{ud}\rho^{R}_{i,l,ud}\cdot R_{i,l,ud,h} + \sum_{d=1}^{Nd}\sum_{l=\sec}\sum_{ud}\rho^{R}_{d,l,ud}\cdot R_{d,l,ud,h} \\ &+ \sum_{s=1}^{Ns}\sum_{l}\pi_s\Bigg(\sum_{i=1}^{Ng}\left[a_i\cdot u^{l}_{i,h} + b_i\cdot P^{s}_{i,l,h}\right] + \rho_w\cdot\sum_{w=1}^{Nw}P^{s}_{w,l,h} \\ &+ \rho_v\cdot\sum_{v=1}^{Nv}P^{s}_{v,l,h} + \sum_{d=1}^{Nd}\rho^{E}_{d}\cdot P^{s}_{d,l,h}\Bigg) + Voll.ELNS_h\Bigg) \end{aligned} \tag{17}$$

where $a_i, b_i, \rho_w, \rho_v, \rho_d^E, \rho_{i,l,ud}^R$ and $\rho_{d,l,ud}^R$ are representing fixed operation cost, first-order operation cost of ith VSI based DG, cost of operation of wind turbine w, cost of operation of photovoltaic panel v, cost of offered energy of dth DRP, cost of up/down reserve of ith VSI based DG in control level l and cost of offered up/down reserve of dth DRP control level l, respectively. $R_{i,l,ud,h}$ and $R_{d,l,ud,h}$ denote scheduled up/down reserve of ith VSI based DG and scheduled up/down reserve of dth DRP in control level l and hour h, respectively. $P_{w,h}$ and $P_{w,h}$ represent forecasted active power output of wind turbine w and forecasted active power output of photovoltaic panel v at hour h, respectively. $P_{d,h}$ expresses aggregated offered load reduction corresponding to dth DRP at hour h. $P_{i,l,h}^s, P_{d,l,h}^s, P_{w,l,h}^s$ and $P_{v,l,h}^s$ show active power output of ith VSI based DG, aggregated offered load reduction corresponding to dth DRP, active power output of wind turbine w and active power output of photovoltaic panel v in scenario s, control level l and hour h, respectively. π_s indicates probability of scenario s and *Voll* explains value of the microgrid lost load. In Eq. (17), the term Expected Load Not Served (*ELNS*) describes the aggregated amount of the expected load shed involuntarily in the considered hierarchical control structure. The second objective function (F_2) is defined as total day-ahead produced emission as follows in Eq. (18):

$$F_2 = \sum_{h=1}^{Nh}\left[\sum_{i=1}^{Ng} E_i^g \cdot P_{i,h} + \sum_{s=1}^{Ns}\sum_{i=1}^{Ng}\sum_{l}\pi_s \cdot E_i^g \cdot P_{i,l,h}^s\right] \tag{18}$$

where E_i^g represents CO_2 emission rate of ith VSI based DG. Absolute value of the microgrid day-ahead expected frequency excursions in the hierarchical control levels is modeled as the third objective function (F_3) as follows in Eq. (19):

$$F_3 = \sum_{s=1}^{Ns}\sum_{h=1}^{Nh}\sum_{l}\pi_s \cdot |\Delta f_{l,h}^s| \tag{19}$$

Besides, the forth objective function consists of the microgrid rate of change of frequency indices as follows in Eq. (20):

$$F_4 = \sum_{s=1}^{Ns}\sum_{h=1}^{Nh}\pi_s \cdot \left[|ROCOF_{MG,h}^s| + \sum_{i=1}^{Ng}|ROCOF_{i,h}^s|\right] \tag{20}$$

2.4.2. Constraints

The developed multi-objective optimization should be solved by means of the MGCC subject to several constraints restricting the microgrid operational planning. Microgrid frequency dependent functions have been thoroughly modeled using Eqs. (1)–(16). Furthermore, to ensure the required static and dynamic securities, the MGCC must manage the microgrid frequency in some secure ranges as described by Eqs. (21)–(23):

$$|\Delta f_{l,h}^s| \leqslant \Delta f_l^{\max},\ l = pri,\ \sec \tag{21}$$

$$|W_{i,h}^s \cdot ROCOF_{i,h}^s| \leqslant W_{i,h}^s \cdot u_{i,h}^l \cdot ROCOF_i^{\max},\ l = pri \tag{22}$$

$$|ROCOF_{MG,h}^s| \leqslant ROCOF_{MG}^{\max} \tag{23}$$

where $\Delta f_l^{max}, ROCOF_{MG}^{max}$ and $ROCOF_i^{max}$ are representing maximum allowable microgrid static frequency excursion limit during control level l, maximum allowable microgrid rate of change of frequency limit and maximum allowable rate of change of frequency limit associated to ith DG, respectively. Other operational constraints corresponding to the DGs and DRPs are comprehensively described in [14,19].

2.5. Energy and frequency security pricing mechanism

In this section, the associated prices of the energy and frequency security are derived out based on the marginal values associated to the hourly power balance equations. The hourly power balance equations of the microgrid in the hierarchical control levels are represented by Eqs. (24) and (25):

$$\sum_{i=1}^{Ng} P_{i,h} + \sum_{w=1}^{Nw} P_{w,h} + \sum_{v=1}^{Nv} P_{v,h} + \sum_{d=1}^{Nd} P_{d,h} = P_{L,h} \tag{24}$$

$$\sum_{i=1}^{Ng} P_{i,l,h}^s + \sum_{w=1}^{Nw} P_{w,l,h}^s + \sum_{v=1}^{Nv} P_{v,l,h}^s + \sum_{d=1}^{Nd} P_{d,l,h}^s = P_{L,l,h}^s + D_{L,l,h}^s \cdot \Delta f_{l,h}^s - LSH_{l,h}^s \tag{25}$$

where $P_{L,h}$ and $P_{L,l,h}^s$ are showing forecasted the microgrid load consumption at hour h and load consumption during scenario s and in control level l, respectively.

According to the method presented in [26,27], the hourly prices of energy and security can be easily obtained as follows in (26) and (27), respectively:

$$\Phi_h^E = \mu_h + \sum_{s=1}^{Ns}\sum_{l}\mu_{l,h}^s \tag{26}$$

$$\Phi_h^S = \sum_{s=1}^{Ns}\sum_{l}\mu_{l,h}^s \tag{27}$$

where μ_h and $\mu_{l,h}^s$ are the Lagrange multiplier corresponding to Eqs. (24) and (25), respectively. While the main objective function is the economic-based one (F_1), the calculated Lagrange multipliers defining the hourly costs of procurement the power balance equalities. Φ_h^E and Φ_h^S are representing the hourly of the microgrid energy and frequency security prices, respectively.

2.6. Multi-objective solution methodology

Principally, in the multi-objective optimization problems instead of achieving a unique optimal solution, the concept of Pareto optimality is introduced [28]. In the Pareto optimal solutions, the optimal solution of an objective function will be achieved by weakening the performance of the other objective functions. Hence, the decision maker has to select the most preferable objective function among the available Pareto optimal solutions owing to its operational policies. One of the efficient multi-objective optimizing solvers is based on well-known augmented epsilon-constraint method.

2.6.1. Augmented epsilon-constraint method

Augmented epsilon constraint methodology is a well known optimization approach, hence, to avoid tautology in writing, in this paper, only the cornerstone formulations of an augmented epsilon-constraint method by minimization target is presented as follows in (28) and (29). More details on this issue can be found in references [29,30].

$$\text{Min}\left(F_1 - r_1 \cdot \sum_{i=2}^{M}\frac{s_i^k}{r_i}\right) \tag{28}$$

s.t.

$$e_i^k = F_i^{\max} - k\frac{r_i}{q_i},\quad s_i \in R^+,\ i = 2, 3, \ldots, M,\ k = 0, 1, \ldots, q_i \tag{29}$$

where M is total number of the Pareto optimal solutions, s_i is an interval variable, r_i is the range of ith objective function and can

be calculated owing to the corresponding payoff table. e_i^k is an iterative variation parameter identified to obtain the Pareto solutions. q_i indicates the number of equal parts ith objective function is divided.

2.6.2. Nash inspired decision making algorithm

In order to simulate the decision making preference, an appropriate reliable strategy should be employed to identify the best compromise solution from the generated Pareto front in the multi-objective optimizations. Some of the applied decision making procedures to the power system optimization problems are included as fuzzy membership function [30], Analytical Hierarchy Process (AHP) [31], Technique for Order Preference by Similarity to Ideal Solution (TOPSIS) [32] and etc. The drawback of fuzzy based decision making approaches is that the trade-off between competitive objective functions is not considered and it stands on experience in the construction of membership functions. In this paper, owing to the analogy between the various objective functions in the multi-objective optimization to a set of non-cooperative players in the game theory, the concept of Pareto optimality selection is proposed to be transformed to a Nash equilibrium point derivation on the basis of the game theory [33]. Thus, each objective function is modeled as a non-cooperative player in the proposed game theory framework in which Nash equilibrium point will be optimized subject to some probability and rationality constraints according to the trade-off between various points in the Pareto front space. The optimized Nash equilibrium point is equivalent to the best compromise solution of the multi-objective problem. The proposed Nash inspired optimization problem to find out the best compromise solution from the augmented epsilon-constraint generated Pareto front space is formulated as in equation set (30):

$$\begin{aligned}
&\text{Min Nash } [Z_1,\ldots,Z_k,\ldots,Z_n,\lambda_1,\ldots,\lambda_k,\ldots,\lambda_n]\\
&\quad=\sum_{k=1}^{n}\left\{\sum_{l=1}^{m}\left(\omega_k F_l^k\right)\cdot\left(\prod_{k=1}^{n} z_l^k\right)\right\}+\sum_{k=1}^{n}\lambda_k\\
&s.t.\\
&\sum_{l=1}^{m} z_l^k=1,\ \forall k=1,2,\ldots,n;\\
&\sum_{l=1}^{m}\left(\omega_k F_l^k\right)\cdot z_l^k\geqslant\lambda_k,\ \forall k=1,2,\ldots,n;\\
&z_l^k\geqslant 0,\ \forall k=1,2,\ldots,n,\forall l=1,2,\ldots,m.
\end{aligned}\tag{30}$$

where n and m are number of total objective functions and number of total generated solution points in the Pareto front set. F_l^k, z_l^k and $Z_k=[z_1^k,z_2^k,\ldots,z_l^k,\ldots,z_m^k]$ represent the kth normalized objective function related to the lth solution in the Pareto front, the kth objective function equilibrium value of the lth solution in the Pareto front and the Nash equilibrium solution point corresponding to the kth objective function, respectively. Z_k is also a vector representing the probability distribution for the objective functions over the Pareto front. Parameter ω_k explains the decision maker relative preference over the considered objective functions in the Pareto front set. The unbiased preference of the decision maker can be mentioned by setting ω_k to 1. Maximum expectation limit related to the kth player has been expressed by λ_k. Obviously, by optimal solving the proposed Nash inspired optimization framework, decision maker, in this paper the MGCC, can derive the best compromise solution which is equivalent to the minimum value of the obtained equilibrium point vector as in can be described by $[\prod_{k=1}^{n} z_1^k,\prod_{k=1}^{n} z_2^k,\ldots,\prod_{k=1}^{n} z_l^k,\ldots,\prod_{k=1}^{n} z_m^k]$.

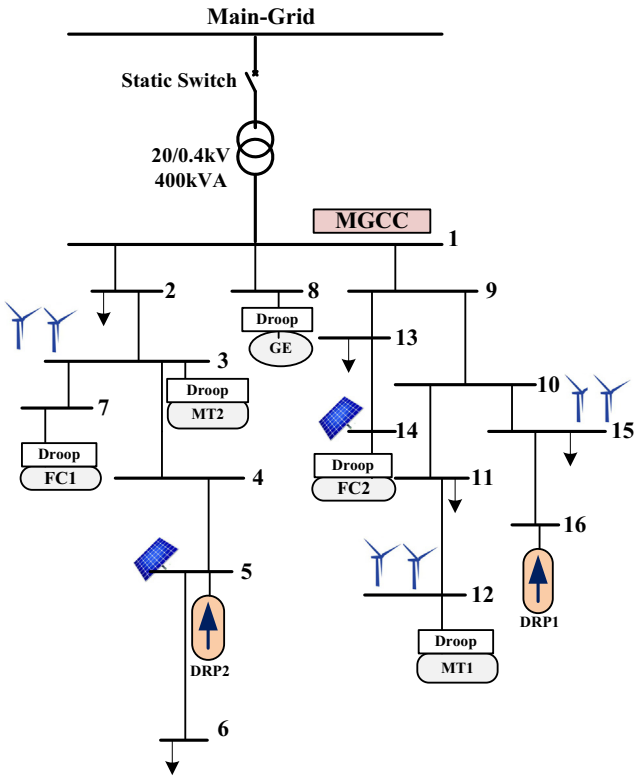

Fig. 4. The simulated microgrid test system.

3. Illustrative implementations

The developed model is analyzed through three case-studies which are all implemented in a typical test microgrid as shown in Fig. 4. The droop controlled DGs consist of two Micro-Turbines (MTs), two Fuel Cells (FCs) and a Gas Engine (GE). Additionally, three similar WT and two PV units are also dispersed in the distribution feeders. Besides, two DRPs are considered to offer the end-user consumer load reduction bids to the MGCC. In cases 1 and 2, the MGCC is in charge to control the microgrid frequency without consideration the demand response resources while in case 3 the DRPs are taken into account. In all case-studies the allowable primary frequency excursion is set at ±350 mHz. In case 2, the MGCC is allowed to manage the microgrid energy and reserves such that the secondary frequency is controlled at a secure range in which ±100 mHz frequency excursion is acceptable. In cases 1 and 3, the MGCC is obliged to provide the frequency security such that the microgrid secondary frequency is controlled at exactly its rated value, i.e. the secondary frequency excursion should be set at zero. The maximum allowable rocof is assumed to be ±1.5 Hz/s for any DG and also for the whole microgrid. Worth to be mentioned that, all data related to the static and dynamic frequency control security ranges have been adopted from IEEE Standard 1547-2003 [34]. Moreover, the operational data of the each type of the DER units in the simulated microgrid test system are taken from [35,36] and listed in Table. 1. Besides, the forecasted values of the microgrid hourly WT/PV active power generation and load consumption are presented in Table. 2 [35]. As shown in Table. 2, the amounts of the active power outputs corresponding to the WT/PV units are listed based on their furcated value per to the installed capacity of the RES units. To calculate the forecast power generation of each WT/PV unit the per capacity data should multiplied by the nominal power capacity of each WT (i.e. 80 kW) or each PV (i.e. 70 kW) unit. Moreover, the

Table 1
The techno-economic data of the microgrid.

DG	Minimum generation limit (kW)	Maximum generation limit (kW)	Fixed cost (cents/h)	Generation cost (cents/kW h)	Start-up cost (cents)	Shut-down cost (cents)	Primary reserve cost (cents)	Secondary reserve cost (cents)	Droop coefficient (mHz/kW)	Emission rate (kg/kW h)
MT	25	150	85.06	4.37	9	8	6.00	2.10	10.0	0.550
FC	20	100	255.18	2.84	16	9	4.00	1.50	15.0	0.377
GE	35	200	212.00	3.12	12	8	3.80	1.70	7.5	0.890
WT	0	80	0	10.63	–	–	–	–	–	–
PV	0	70	0	54.84	–	–	–	–	–	–

Table 2
Hourly forecasted values of Wind/PV active powers and load consumption.

Hour	Wind power (kW/installed kW)	PV (kW/installed kW)	Load consumption (kW)
1	0.364	0	286
2	0.267	0	275
3	0.267	0	273
4	0.234	0	280
5	0.312	0	310
6	0.329	0	315
7	0.476	0.002	327
8	0.477	0.008	332
9	0.424	0.035	350
10	0.381	0.100	388
11	0.459	0.230	430
12	0.390	0.233	466
13	0.494	0.318	500
14	0.355	0.433	512
15	0.433	0.370	500
16	0.321	0.403	537
17	0.329	0.330	557
18	0.303	0.238	600
19	0.364	0.133	660
20	0.373	0.043	630
21	0.260	0.003	600
22	0.338	0	520
23	0.312	0	477
24	0.346	0	400

microgrid loads are assumed to be aggregated in a single node and thus the microgrid whole consumption can be forecasted as listed in Table. 2. The proposed step-wise price-demand curves of the two DRPs are listed in Table. 3. The value of lost load is assumed to be 1000 cents/kW h. In this study, first 1000 scenarios consist of the microgrid aggregated load consumptions, WT/PV power outputs and availability status of the DGs are derived using the proposed MCS and RWM strategies. The finally remained scenario numbers after the implementation of a proper scenario reduction algorithm are 20. The reduced scenarios have been applied to the proposed MILP stochastic optimization model. The multi-objective optimization is aimed to be solved in a 24 h time horizon.

The pre-defined four-fold objective functions are considered to be optimized simultaneously in the proposed hierarchical multi-objective frequency management framework. The proposed multi-objective programming based on augmented epsilon constraint method is adopted to make a compromise between the one economical (F_1), one environmental (F_2) and two technical frequency dependent (F_3 and F_4) objectives. The calculated payoff tables are presented by ψ_1, ψ_2 and ψ_3 corresponding to cases 1, 2 and 3, respectively.

Table 3
Price-demand offered package of the DRPs.

DRP1	Demand (kW)	0–25	25–65	65–95	95–120
	Offered Price (cents)	0.3	0.48	0.60	0.75
DRP2	Demand (kW)	0–40	40–60	60–85	85–135
	Offered Price (cents)	0.25	0.45	0.65	0.80

$$\psi_1 = \begin{pmatrix} 267613.968 & 15623.305 & 3.940 & 55.203 \\ 10303951.881 & 7094.761 & 8.399 & 128.489 \\ 7122519.927 & 11636.822 & 0.440 & 8.946 \\ 7022368.163 & 12054.830 & 1.218 & 8.438 \end{pmatrix};$$

$$\psi_2 = \begin{pmatrix} 266609.360 & 15623.433 & 4.680 & 56.637 \\ 10298966.116 & 7188.008 & 8.382 & 127.354 \\ 6853943.148 & 12187.303 & 0.444 & 8.620 \\ 6277873.496 & 12544.522 & 1.445 & 8.437 \end{pmatrix};$$

$$\psi_3 = \begin{pmatrix} 195336.934 & 7750.798 & 4.869 & 55.853 \\ 9733233.521 & 2253.142 & 6.334 & 59.734 \\ 7315186.641 & 5945.851 & 0.442 & 8.981 \\ 6836395.906 & 6848.979 & 1.960 & 8.437 \end{pmatrix}$$

The multi-objective optimization results associated to the non-inferior feasible solutions are listed in Table 4 for different case-studies. Worth mentioning that main objective function is the economical one (F_1) and the optimization procedure is solved subject to that other objective functions have been constrained.

Predictably, decrease in the environmental objective (F_2) causes the microgrid operational costs to be increased. On other hand, decrease in the frequency security objectives (F_3 and F_4) must result in much higher operational costs which are due to the higher microgrid security improvement. Totally, changes in the operational cost objective function (F_1) are resultants of superposition of changes in values and directions of the other objective functions (F_2, F_3 and F_4). For example, in case 1, in Pareto point 6 although F_3 objective has been increased with respect to point 5, F_1 has been increased because of decreases in F_2 and F_4 functions. Similarly, a considerable decrease in environmental and static frequency security objectives in case 2, point 7 with respect to point 6 makes a significant increase in F_1 function. The notable decreases in F_3 and F_4 functions, in case 3, point 5 comparing to point 4, leads the F_1 objective to be increased considerably.

To select the best compromise solution from the generated Pareto points, the proposed Nash inspired decision making algorithm has been applied to the generated Pareto points in Table 4. The selected Pareto point in cases 1, 2 and 3 is the 8th, 8th and 10th ones, respectively as shown distinctively in Table. 4. Observably, in case 3 where the demand response resources have been implemented total operational costs of the microgrid has been decreased from 2347367.907 in case 1 to 910786.332 in case 3 cents Day^{-1}. Besides, in case 2 in which the MGCC is not obliged to regulate the secondary frequency at exactly its rated value, the operational cost has been decreased within 84689.112 cents Day^{-1}. In the following, for the best selected compromise solutions, the breakdown of the associated operational cost and emission levels corresponding to cases 1, 2 and 3 have been represented in Table 5.

Table 4
The multi-objective optimization results corresponding to the generated Pareto front in cases 1, 2 and 3 (the selected best compromise solutions are specified in bold).

Case	Case 1				Case 2				Case 3			
Pareto point	F_1 (cent)	F_2 (kg)	F_3 (Hz)	F_4 (Hz/s)	F_1 (cent)	F_2 (kg)	F_3 (Hz)	F_4 (Hz/s)	F_1 (cent)	F_2 (kg)	F_3 (Hz)	F_4 (Hz/s)
1	268728.46	15623.30	5.14	80.67	267855.44	15623.43	4.72	56.68	195073.25	7474.43	4.79	56.10
2	269464.44	14912.59	5.21	79.78	268917.54	14920.48	5.99	80.92	195556.89	7104.09	5.24	55.46
3	274122.88	14201.88	4.61	74.72	270490.89	14217.53	5.42	73.23	203088.63	6834.52	5.35	51.18
4	275133.95	13491.17	4.49	98.47	273218.80	13514.57	6.39	97.62	261259.32	6834.52	4.96	47.91
5	289917.60	12780.45	5.07	88.47	282715.11	12811.62	5.73	87.71	376215.62	5918.24	4.37	42.63
6	391256.82	12069.74	5.08	78.46	379016.37	12108.67	5.07	77.80	473101.00	5460.18	3.88	38.36
7	975600.44	11359.03	4.41	68.46	922041.08	11405.72	4.03	67.89	577393.96	5001.97	3.38	34.08
8	**2105074.65**	**10648.32**	**1.62**	**21.48**	**2006560.69**	**10702.77**	**1.88**	**21.44**	687530.88	4543.83	2.89	29.81
9	3392499.34	9937.61	1.63	21.45	3279627.16	9999.82	1.63	21.72	806071.30	4085.69	2.40	25.53
10	4741471.90	9226.89	2.43	34.15	4628308.07	9296.86	2.42	33.68	**960909.93**	**3627.55**	**1.91**	**21.26**
11	6624520.24	8516.18	1.76	26.07	6507919.20	8593.91	1.77	26.10	1636514.06	3169.41	1.42	12.86

Table 5
The breakdown of associated costs and emissions corresponding to the best compromise solutions.

Case	Operational costs (cents)								ELNS (kWh)	Operational emissions (kg)
	Provided energy		Scheduled reserve			Expected deployed reserve				
	DG	DR	Primary	Secondary		Primary	Secondary			
			DG	DG	DR	DG	DG	DR		
1	43562.392	–	5774.146	6458.606	–	42409.061	42124.491	–	2098.964	3628.013
2	43562.392	–	5775.066	6322.001	–	42533.911	42381.830	–	2013.936	3628.013
3	26592.641	2130.664	7229.935	3839.438	57.358	26631.39	28274.530	2167.845	715.411	2241.044

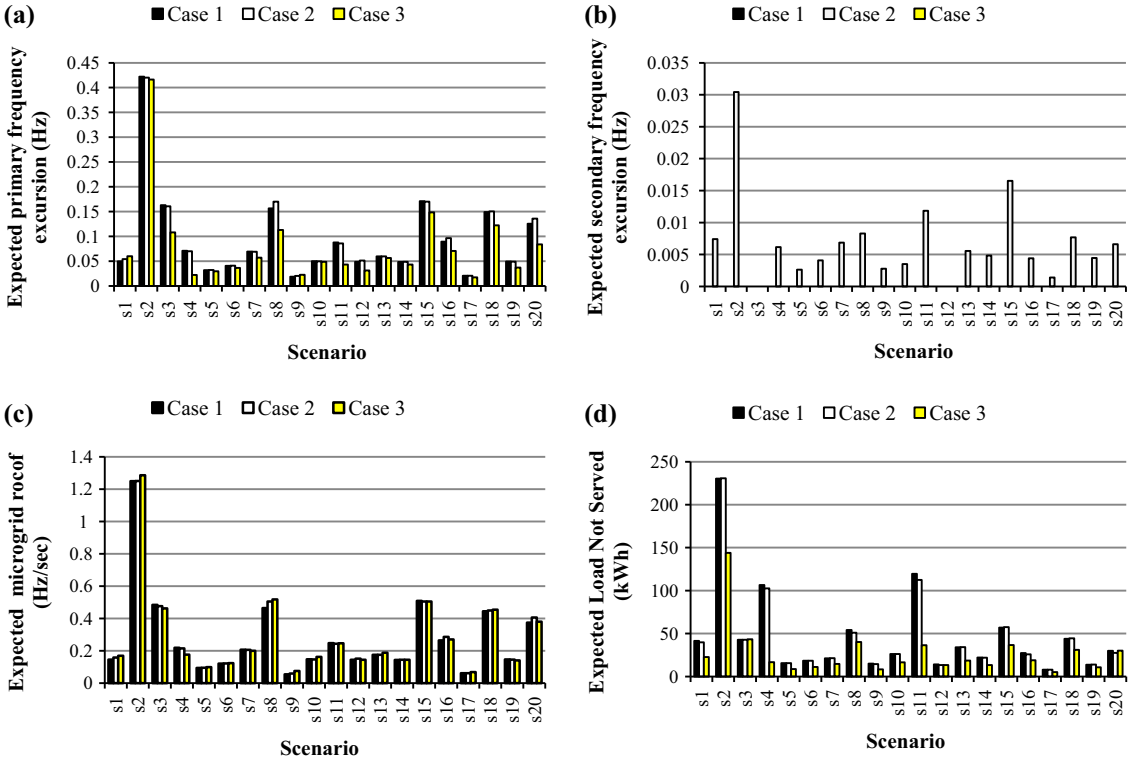

Fig. 5. Expected absolute values of the microgrid primary (a), secondary (b) frequency excursions, rocof (c) and load not served (d) in the reduced scenarios.

Observably as indicated in Table. 5, the costs of provided energy and also amounts of produced emissions by means of the DGs have been decreased significantly when the demand response resources are participated. Furthermore, in case 2, in which the ±100 mHz secondary frequency excursion is allowed, the MGCC has higher degrees of freedom to better utilization of available DGs in providing energy and reserves. Despite the operational costs associated to the provided energy and scheduled primary control reserves have been increased in case 2 comparing to case 1, by better management the stored electrical energy of the DGs, the amounts of the involuntary load shedding have been decreased within 85.04 kW Day^{-1}. Therefore, the total operational costs of the microgrid have been decreased in case 2. Besides, in case 2 with respect to case 1, due to higher allowable frequency excursion, the MGCC can manage the secondary frequency control reserves more economically by appropriately regulating the

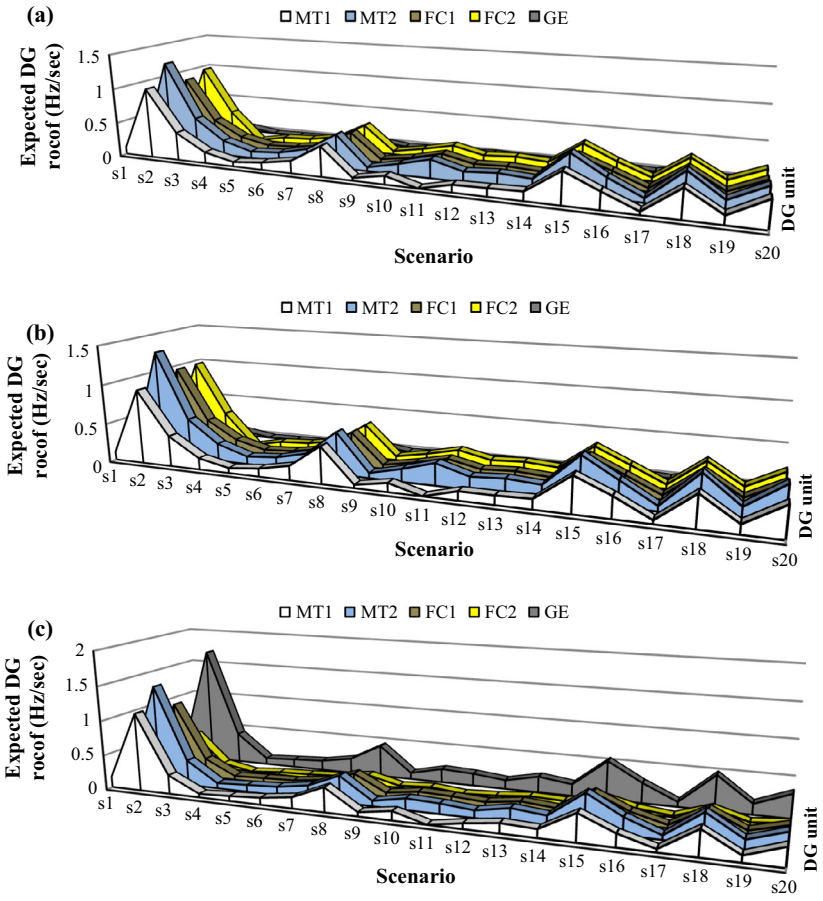

Fig. 6. Expected absolute values of available DG rocof in case 1 (a), case 2 (b) and case 3 (c).

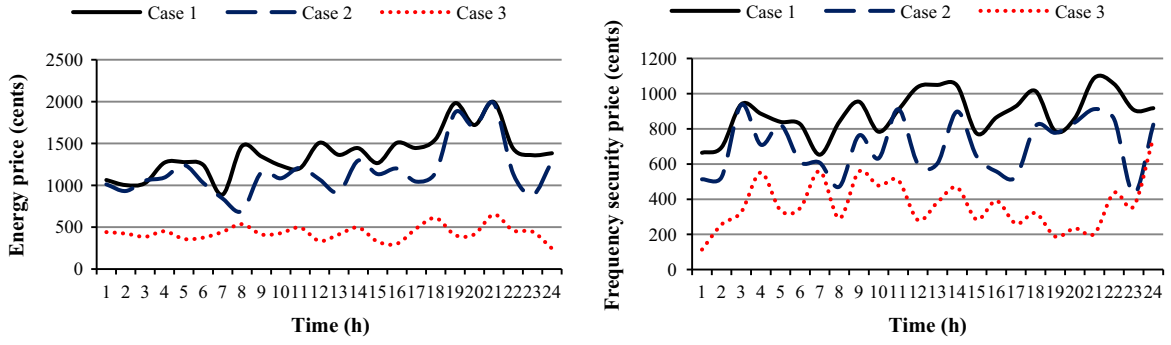

Fig. 7. Hourly energy and frequency security prices.

reference active power set-points of the DGs. The expected values of primary, secondary frequency excursions, expected value of rate of change of the microgrid frequency and also expected load not served are depicted in Fig. 5 for the 20 reduced remained scenarios. As indicated in Fig. 5, the microgrid experiences lower static frequency excursions and lower load shedding in case 3 in the light of taken the demand response resources into account. However, the multi-objective optimization results in higher dynamic frequency excursions in case 3. Moreover, the MGCC by adopting a more risky frequency management policy in case 2, the amounts of both the primary, secondary and rocof indices has increased in comparison of case 1. However, as indicated in Table 4, in case 2, based on reduction the expected amount load not served (*ELNS*), the microgrid static and dynamic frequencies have been managed securely with lower operational cost with respect to case 1. The amounts of dedicated expected values of microgrid secondary frequency excursions on basis of the optimal reference active power set-points of the DGs in all scenarios are depicted in Fig. 5b. The allowable secondary frequency excursion causes the upward secondary control reserves are provided by lower costs. The MGCC has this authority to optimistically determine the secondary frequency excursion in each scenario such that both the security and economical issues are satisfied. For example, in some scenarios such s3 and s12, it is not necessary to allow the microgrid frequency to be deviated from the nominal value. In contrast in some scenarios higher secondary frequency excursions have been applied based on the MGCC decision makings.

The expected absolute values of the committed DG rate of change of frequency index have been represented in Fig. 6. In case 3, by optimal participation of the DRPs, the inexpensive DGs, i.e. the GE have been dispatched more than the other available DGs such as FCs or MTs, thus the expected amounts of the rate of change of frequency of the GE are higher. As it can be observed in scenarios s4 and s11, the FC2 and MT1 units, respectively, have been out of service for a 24 h time horizon. Thus, the amounts of the corresponding expected ROCOFs equal to zero in all cases.

Lastly, the hourly prices of the energy and frequency security are derived out by implementing Eqs. (27) and (28). The energy and security prices are shown in Fig. 7. Again, the energy and security prices are lower in case 3 comparing to the cases 1 and 2. Predictably, in case 1, when the MGCC applies a more conservative strategy, consequently the hourly prices of energy and frequency security are greater with respect to case 2. The developed MILP model is solved using CPLEX as a powerful solver under the GAMS environment [37] on a platform with Intel Core i5-4660 CPU and 8 GB of RAM. It should be mentioned that the execution time corresponding to the proposed multi-objective optimization procedures in cases 1, 2 and 3 are 422, 436 and 518 sec, respectively.

4. Conclusions

The paper proposed a novel energy and frequency security pricing mechanism for islanded droop controlled microgrids. The problem has been formulated as a multi-objective energy management system which was aimed to be solved using the augmented epsilon constraint optimization method. The best compromise solution has been selected using a novel Nash inspired equilibrium point decision making approach. The optimization results were implemented over three different case-studies in accordance to the MGCC operational policies. The hourly energy and frequency security prices have been derived out based on the specification of the associated Lagrange multipliers of the hourly power balance equations. Analyzing the results verifies that adopting a conservative operational policy in which the MGCC was obliged to restore the microgrid frequency at exactly its rated value imposes higher operational cost and emission levels. On the other hand, taking the demand response resources into account lowers the hourly prices of the energy and security significantly. Furthermore, day-ahead energy and reserve resources are scheduled appropriately under a well-organized stochastic programming framework. The effectiveness of the proposed equilibrium inspired multi-objective decision making approach in selecting the best compromise solution is shown based on a nonlinear optimization. The proposed model can reconcile the insight view for the MGCC in determining appropriate operational policies to ensure frequency security requirements of islanded microgrids which also justifies the economic-environmental objectives.

References

[1] Katiraei F, Iravani R, Hatziargyriou N, Dimeas A. Microgrids management. IEEE Power Energy Mag 2008;6(3):54–65.
[2] Rabbanifar P, Jadid S. Stochastic multi-objective security constrained market clearing considering static frequency of power systems. Int J Electr Power Energy Syst 2014;54:465–80.
[3] Olivares DE, Canizares CA, Kazerani M. A centralized energy management system for isolated microgrids. IEEE Trans Smart Grid 2014;5(4):1864–75.
[4] Jimeno J, Anduaga J, Oyarzabal J, de Muro AG. Architecture of a microgrid energy management system. Eur Trans Elect Eng 2011;21:1142–58.
[5] Chen C, Duan S, Cai T, Liu B, Hu G. Smart energy management strategy for optimal microgrid economic operation. IET Renew Power Gener 2011;5(3):258–67.
[6] Mohammad FA, Koivo HN. Online management genetic algorithms of microgrid for residential application. Energy Convers Manage 2012;64:562–8.
[7] Abdolaziz MMA, El-Saadany EF. Maximum loadability consideration in droop controlled islanded microgrids optimal power flow. Electr Power Syst Res 2014;106:168–79.
[8] Conti S, Nicolosi R, Rizzo SA, Zeineldin HH. Optimal dispatching of distributed generators and storage systems for MV islanded microgrids. IEEE Trans Power Delivery 2012;27(3):1243–51.
[9] Mohammadi S, Mozafari B, Solymani S, Niknam T. Stochastic scenario-based model and investigating size of energy storages for PEM-fuel cell unit commitment of microgrid considering profitable strategies. IET Gener Transm Distrib 2014;8(7):1228–43.
[10] Guo L, Liu W, Jiao B, Hong B, Wang C. Multi-objective stochastic optimal planning method for stand-alone microgrid. IET Gener Transm Distrib 2014;8(7):1263–73.
[11] Marzband M, Sumper A, Garcia JLD, Ferret RG. Experimental validation of a real time energy management system for microgrids in islanded mode using a local day-ahead electricity market and MINLP. Energy Convers Manage 2013;76:314–22.
[12] Mazidi M, Zakariazadeh A, Jadid S, Siano P. Integrated scheduling of renewable generation and demand response programs in a microgrid. Energy Convers Manage 2014;86:1118–27.
[13] Zakariazadeh A, Jadid S, Siano P. Economic-environmental energy and reserve scheduling of smart distribution systems: a multi-objective mathematical programming approach. Energy Convers Manage 2014;78:151–64.
[14] Rezaei N, Kalantar M. Economic-environmental hierarchical frequency management of a droop controlled islanded microgrid. Energy Convers Manage 2014;88:498–515.
[15] Rezaei N, Kalantar M. Smart microgrid hierarchical frequency control ancillary service provision based on virtual inertia concept: an integrated demand response and droop controlled distributed generation framework. Energy Convers Manage 2015;92:287–301.
[16] Rocabert J, Luna A, Blaabjerg F, Rudriguez P. Control of power converters in AC microgrids. IEEE Trans Power Electron 2012;27(11):4734–49.
[17] Lopez JAP, Moreira CL, Madureira AG. Defining control strategies for microgrids islanded operation. IEEE Trans Power Syst 2006;21(2):916–24.
[18] Guerrero JM, Chandorkar M, Lee TL, Loh PC. Advanced control architecture for intelligent microgrids-part I: decentralized and hierarchical control. IEEE Trans Industr Electron 2013;60(4):1254–62.
[19] Rezaei N, Kalantar M. Stochastic frequency-security constrained energy and reserve management of an inverter interfaced islanded microgrid considering demand response programs. Int J Electr Power Energy Syst 2015;69:273–86.
[20] Faria P, Vale Z. Demand response in electrical energy supply: an optimal real time pricing approach. Energy 2011;36:5374–84.
[21] Palensky P, Dietrich D. Demand-side management: demand response, intelligent energy systems and smart loads. IEEE Trans Industr Inf 2011;7(3):381–8.
[22] Siano P. Demand response and smart grids-A survey. Renew Sustain Energy Rev 2014;30:461–78.
[23] Wu L, Shahidehpour M, Li T. Cost of reliability analysis based on stochastic unit commitment. IEEE Trans Power Syst 2008;23(3):1364–74.
[24] Billinton R, Allan RN. Reliability evaluation of power systems. New York, USA: Plenum; 1996.
[25] Esmaili M, Amjady N, Shayanfar HA. Stochastic congestion management in power markets using efficient scenario approaches. Energy Convers Manage 2010;51:2285–93.
[26] Arroyo JM, Galiana FD. Energy and reserve pricing in security and network constrained electricity markets. IEEE Trans Power Syst 2005;20(2):634–43.
[27] Jadid S, Rabbanifar P. Stochastic multi-objective frequency control in joint energy and reserve markets considering power system security. IET GenTrans Distrib 2013;7(1):76–89.
[28] Ahmadi A, Aghaei J, Shayanfar HA, Rabiee A. Mixed integer programming of multi-objective hydro-thermal self-scheduling. Appl Soft Comput 2012;12(8):2137–46.
[29] Mavrotas G. Effective implementation of the epsilon-constraint method in multi-objective mathematical programming problems modified augmented. Appl Math Comput 2009;213(2):455–65.
[30] Aghaei J, Amjady N, Shayanfar HA. Multi-objective electricity market clearing considering dynamic security by lexicographic optimization and augmented epsilon constraint method. Appl Soft Comput 2011;11(4):3846–58.
[31] Mavalizadeh H, Ahmadi A. Hybrid expansion planning considering security and emission by augmented epsilon-constraint method. Int J Electr Power Energy Syst 2014;61:90–100.
[32] Falsafi H, Zakariazadeh A, Jadid S. The role of demand response in single and multi-objective wind-thermal generation scheduling: a stochastic programming. Energy 2014;64:853–67.
[33] Zhou B, Chan KW, Yu T, Chung CY. Equilibrium inspired multiple group search optimization with synergistic learning for multiobjective electric power dispatch. IEEE Trans Power Syst 2013;28(4):3534–45.
[34] IEEE Standard for interconnecting distributed resources to electric power systems, IEEE Standard 1547-2003.
[35] Tsikalakis AG, Hatziargyriou ND. Centralized control for optimizing microgrids operation. IEEE Trans Energy Convers 2008;23(1):241–8.
[36] Shi L, Luo Y, Tu GY. Bidding strategy of microgrid with consideration of uncertainty for participating in power market. Int J Electr Power Energy Syst 2014;59:1–13.
[37] Generalized Algebraic Modeling Systems (GAMS). <http://www.GAMS.com>.